Photophysics of Tryptophan in Bacteriophage T4 Lysozymes†

Danni L. Harris and Bruce S. Hudson*

Department of Chemistry and Institute of Molecular Biology, University of Oregon, Eugene, Oregon 97403

Received December 7, 1989; Revised Manuscript Received February 14, 1990

ABSTRACT: Bacteriophage T4 lysozyme contains three tryptophan residues in distinct environments. Lysozymes with one or two of these residues replaced by tyrosine are used to characterize the photophysics of tryptophan in these individual sites. The fluorescence spectra, average lifetimes, and quantum yields of these three single-tryptophan variants are understandable in terms of the neighboring residues. The emission spectra and radiative lifetimes are found to be the same for all three species while the quantum yield and decay kinetics are quite distinct. The variation of the average nonradiative rate constant is correlated with neighboring quenching groups. Quenching by I^- correlates with exposure of the tryptophan residue based on the crystal structure. Complex behavior is observed for the time dependence of the fluorescence decay in all three cases, including that of the immobile tryptophan-138 residue. The complexity of the fluorescence decay is ascribed to heterogeneity in the nonradiative rate constant among microstates. Energy transfer between tryptophan residues is inferred to occur from comparison of the quantum yields of the two-tryptophan and single-tryptophan proteins and is discussed in terms of the Förster mechanism.

Fluorescence studies of proteins often provide useful information regarding the environment and dynamics of the region surrounding naturally occurring fluorescent amino acids. There have been several recent studies of the fluorescence of proteins containing single tryptophan residues (Petrich et al., 1987; Eftink & Ghiron, 1987; Gryczynski et al., 1988; Chen et al., 1987; MacKerell et al., 1987; Ludescher et al., 1987; Hudson et al., 1987a). The interpretation of protein tryptophan fluorescence lifetime data is a continuing challenge (Creed, 1984; Beechem & Brand, 1985). Explanations of the complex photophysics of tryptophan have been related to solvent relaxation (Lakowicz et al., 1988; Lami & Glasser, 1986; Gonzalo & Montoro, 1985; Gudgin-Templeton & Ware, 1984; Grinvald & Steinberg, 1974a), including exciplex formation (Mattes & Farid, 1984; Herschberger et al., 1981) and dynamic quenching (Tanaka & Mataga, 1987) as well as conformational heterogeneity (Petrich et al., 1983; Szabo & Rayner, 1980). An understanding of the source of tryptophan fluorescence lifetime heterogeneity is crucial to complete interpretation of polarization anisotropy data (Hudson et al., 1987b; Ludescher et al., 1987). An association between lifetime components and physical (or "chemical") species is often problematical even for cases of small molecules in solution (James & Ware, 1985a,b). In many cases, lifetime heterogeneity is sufficiently complex that it is better described as a continuous distribution. This is often appropriate in the case of the lifetime description for tryptophans in a protein (Alcala et al., 1987). Part of the lifetime complexity of tryptophan residues in proteins may be explained by postulating that the chromophores exist in a heterogeneous population of protein conformational substrates as defined by Frauenfelder and co-workers (Austin et al., 1974).

T4 phage lysozyme is a monomeric 164-residue, 18 700-dalton globular protein with no disulfide bridges. The protein has a two-lobed structure with an active-site cleft. The structure of the wild-type (WT) enzyme has been refined to 1.7-Å resolution (R = 0.193) with the inclusion of isotropic thermal parameters (Weaver & Matthews, 1987). A large library of T4 lysozyme variants with single or multiple amino acid replacements is available in an overproducing expression system. Many of these lysozymes have been crystallized and their structures determined (Grütter et al., 1983; Alber et al., 1986). In addition to a well-defined set of crystal structures, thermodynamic, proteolytic digestion, NMR, and hydrogen-exchange measurements have been applied to further characterize the wild-type and variant lysozymes. Some of this work is described in recent review articles.

T4 phage lysozyme (T4L) is an excellent system on which to focus the techniques of time-resolved fluorescence to correlate the effects of amino acid environment with observed tryptophan photophysics and dynamics. In this way, we have begun to establish the nature of the effects of environment on the regions local to each of the three naturally occurring tryptophans in this protein. To simplify the initial work, we have studied three lysozyme variants with all combinations of two of the tryptophan residues replaced by tyrosines. This enables us to make careful characterizations of the fluorescence of a single tryptophan in three unique environments in the same protein without the complications of multi-tryptophan fluorescence. Two of the tryptophans, W126 and W158, are surface residues while W138 is largely buried. All three of these groups exist in quite polar amino acid environments and have adjoining amino acids that are moderate or strong quenchers of tryptophan fluorescence. The present work presents the results of a careful analysis of the fluorescence of these three single-tryptophan proteins.

The study of three lysozyme variants in which one of the three tryptophans found in wild-type T4L has been replaced by tyrosine permits the study of Förster energy transfer for a known geometry. One of the two-tryptophan variants, W126Y, has been crystallized and its structure solved.[1] The structure of this lysozyme is almost isomorphous with the wild-type T4L, indicating the perturbation of the structure due to substitution of tyrosine for tryptophan is minimal. The

† Supported by NIH Grant GM36578.

* To whom correspondence should be addressed.

[1] The construction and characterization of these proteins will be presented in a subsequent publication (L. McIntosh, unpublished results).

0006-2960/90/0429-5276$02.50/0

comparison of the fluorescence properties of multi-tryptophan lysozymes, with amino acid substitutions proximate to one of the three tryptophans, serves as an additional test of hypotheses concerning the role of neighboring amino acids as quenchers of tryptophan fluorescence.

Materials and Methods

Materials. T4 phage lysozymes with tryptophan to tyrosine replacements were obtained from Lawrence McIntosh and Cynthia Phillips, Institute of Molecular Biology, University of Oregon.[1] Amino acids and *N*-acetyltryptophan were obtained from Sigma, Inc. (St. Louis, MO). Acrylamide and β-mercaptoethanol were obtained from Bio-Rad (Richmond, CA).

Sample Preparation. Samples with tryptophan absorbance of ca. 0.1 ODU (300 nm) were prepared by diluting concentrated protein samples into 0.1 M sodium phosphate buffer, pH 6.1. Additional NaCl was added to adjust the ionic strength of the final solutions to 0.2 M. Sufficient β-mercaptoethanol was added to obtain a concentration of 10^{-3} M. KI fluorescence quenching experiments were performed with additional aliquots of KCl solution to maintain constant ionic strength (μ = 2.3 M) and constant enzyme dilution. The former was crucial since it was found that the quantum yield of the T4L variants varied with ionic strength. *N*-Acetyltryptophan solutions were prepared to be pH 5 (0.01 M acetate buffer) and 0.1 M NaCl. The final concentration used for fluorescence was adjusted so that the solution was 0.1 ODU at 300 nm. Stock solutions of amino acids for *N*-acetyltryptophan quenching experiments were ca. 0.25–0.3 M and were prepared in acetate buffer.

Fluorescence Instrumentation. Absorption spectra of lysozymes were recorded on a Varian Model DMS-300 double-beam visible–UV spectrophotometer between 250 and 350 nm. Corrected fluorescence emission spectra were obtained with an SLM-8000 spectrofluorometer (SLM Industries, Urbana, IL). The quantum yields for the T4L variants were determined from the integrated spectra and the quantum yield for tryptophan of 0.12 at pH 6 (Chen, 1972). Fluorescence measurements were obtained by time-resolved single photon counting (O'Connor & Phillips, 1984). Detailed descriptions of the instrumentation and data collection procedures have been described elsewhere (Ruggiero & Hudson, 1989). The frequency-doubled output of a Spectra-Physics 3640 mode-locked Nd:YAG laser was used to synchronously pump a rhodamine 6G dye laser that was cavity dumped at 0.8 MHz. A Hamamatsu R1564U proximity-focused 12-μm microchannel plate was used as a detector. The instrument response function was typically 90-ps full width at half-maximum. Fluorescence excitation was generally at 295 or 300 nm with emission collected from 320 to 420 nm through Corion 10 nm band-pass interference filters. Data collection times were gauged so as to result in a total of several million counts.

Data Analysis Methods: Multiexponential Analysis. In a common form of data analysis, the decay in the fluorescence intensity, $I(t)$, is given by

$$I(t) = I_0 \sum_{i=1}^{n} \alpha_i e^{-(t/\tau_i)} \qquad (1)$$

where α_i is a parameter determining the fractional contribution of the ith exponential to the total fluorescence decay ($\sum_i^n \alpha_i = 1$) and τ_i is the lifetime parameter associated with this term. Time-resolved fluorescence data were analyzed via this multiexponential form by nonlinear least-squares iterative reconvolution (Grinvald & Steinberg, 1974b). The quality of the parameterizations was judged by reduced χ^2, runs tests, weighted residuals, and the autocorrelation of the weighted residuals. As shown, the average lifetime

$$\langle \tau \rangle = \sum_{i=1}^{n} \alpha_i \tau_i \qquad (2)$$

is often the only physically meaningful parameter in such analyses. Analyses of several data sets obtained at different emission wavelengths were also analyzed in a "global" fashion (Beechem et al., 1985) in which the component lifetimes were optimized subject to the constraint that the same values of τ apply to all of the data sets. The variation of the amplitudes in such an analysis reflects the relative contribution of each component to the decay at that emission wavelength.

Distribution Models of Fluorescence Decays. James and Ware (1986) have proposed the use of an analysis that is a discretized distribution employing a large number of exponential terms. Explicitly it takes the form:

$$I(t) = \int \alpha(\tau) e^{-(t/\tau)}\, d\tau \approx \sum_{k=1}^{N} \alpha_k e^{-(t/\tau_k)} \qquad (3)$$

where a large number of fixed, equally spaced lifetime components are used to approximate a continuous distribution by variation of the amplitude factors. The procedure employed involves the use of a large number of exponential terms which, as the analysis proceeds, are reduced in number by eliminating those contributions that are less than 0.5% of the maximum amplitude. The James and Ware procedure should result in a set of isolated components if the fluorescence decay is due to a few distinct species (James & Ware, 1986).

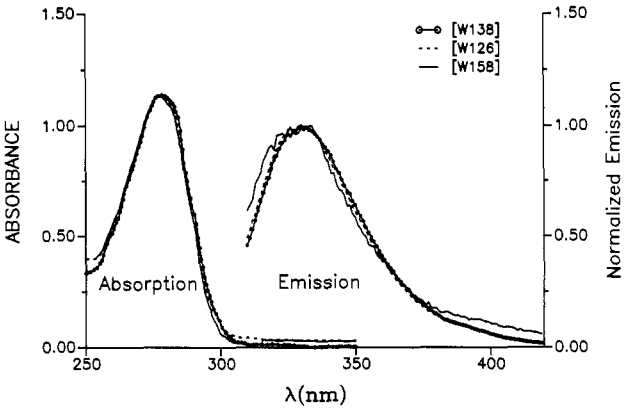

FIGURE 1: Emission (scaled to coincide at spectral maxima) and absorption spectra of single-tryptophan variants of T4 phage lysozyme. (o) [W138]; (---) [W126]; (—) [W158].

Results

Absorption and Emission Spectra. The absorption and (scaled) emission spectra of the single-tryptophan lysozymes are shown in Figure 1. The spectra are virtually identical, with absorption maxima of 278 nm and emission maxima of 330 nm for all three single-tryptophan species, despite the fact that each of these tryptophans is in a unique environment. The emission spectrum of the WT protein is, aside from scaling factors, virtually identical with the spectra of any and all of the single-tryptophan variants. It has also been determined that there is no shift in the emission spectrum of the wild-type protein when potassium iodide is added. Since differential quenching of the residues occurs, this further indicates that the three tryptophan residues of the wild-type species have the same spectra.

Analysis of Fluorescence Data of Single-Tryptophan Variants. Fluorescence intensity decay data for the three

Table I: Discrete Exponential Analysis of Fluorescence Decays: Emission Dependence of [W126] and [W138][a]

variant	λ_{em}	α_1	τ_1	α_2	τ_2	α_3	τ_3	χ^2	$\langle\tau\rangle$
[W126]	320	0.11 ± 0.03	0.58 ± 0.09	0.39 ± 0.03	1.6 ± 0.1	0.50 ± 0.05	2.6 ± 0.04	1.2	2.0
	340	0.12 ± 0.01	0.49 ± 0.05	0.46 ± 0.06	1.8 ± 0.1	0.43 ± 0.07	2.7 ± 0.06	1.1	2.0
	360	0.09 ± 0.02	0.52 ± 0.07	0.41 ± 0.04	1.7 ± 0.1	0.50 ± 0.05	2.7 ± 0.04	1.1	2.1
	380	0.10 ± 0.009	0.50 ± 0.053	0.59 ± 0.043	1.9 ± 0.071	0.31 ± 0.052	3.0 ± 0.08	1.0	2.1
	400	0.14 ± 0.006	0.52 ± 0.03	0.80 ± 0.006	2.2 ± 0.03	0.06 ± 0.01	4.8 ± 0.2	1.1	2.2
	420	0.18 ± 0.006	0.42 ± 0.02	0.74 ± 0.004	2.2 ± 0.02	0.08 ± 0.007	5.7 ± 0.2	1.0	2.2
[W138]	320	0.25 ± 0.007	0.38 ± 0.01	0.66 ± 0.006	1.2 ± 0.01	0.10 ± 0.003	3.2 ± 0.02	1.2	1.2
	340	0.19 ± 0.007	0.37 ± 0.02	0.67 ± 0.007	1.2 ± 0.01	0.14 ± 0.003	3.2 ± 0.02	1.1	1.3
	360	0.15 ± 0.007	0.35 ± 0.02	0.69 ± 0.007	1.2 ± 0.01	0.17 ± 0.003	3.2 ± 0.02	1.0	1.4
	380	0.16 ± 0.02	0.51 ± 0.04	0.66 ± 0.02	1.3 ± 0.02	0.18 ± 0.004	3.4 ± 0.02	1.1	1.5
	400	0.22 ± 0.02	0.60 ± 0.04	0.61 ± 0.02	1.4 ± 0.03	0.17 ± 0.005	3.7 ± 0.03	1.0	1.6
	420	0.29 ± 0.03	0.71 ± 0.04	0.57 ± 0.03	1.6 ± 0.04	0.14 ± 0.005	4.4 ± 0.05	1.0	1.8

[a] λ_{ex} = 300 nm, pH 6, μ = 0.2 M.

Table II: Discrete Exponential Analysis of Fluorescence Decays: Emission Dependence of [W158][a]

λ_{em}	α_1	τ_1	α_2	τ_2	α_3	τ_3	α_4	τ_4	χ^2	$\langle\tau\rangle$
320	0.19 ± 0.007	0.091 ± 0.006	0.69 ± 0.007	0.33 ± 0.003	0.11 ± 0.003	1.01 ± 0.01	0.006 ± 0.0	3.88 ± 0.05	1.7	0.38
340	0.20 ± 0.01	0.12 ± 0.004	0.68 ± 0.01	0.35 ± 0.005	0.12 ± 0.004	1.05 ± 0.02	0.009 ± 0.0	4.42 ± 0.04	1.7	0.42
360	0.21 ± 0.009	0.10 ± 0.007	0.66 ± 0.009	0.36 ± 0.005	0.11 ± 0.003	1.12 ± 0.02	0.014 ± 0.0	4.67 ± 0.04	1.2	0.44
380	0.27 ± 0.01	0.12 ± 0.007	0.61 ± 0.01	0.38 ± 0.006	0.10 ± 0.003	1.34 ± 0.03	0.023 ± 0.0	5.04 ± 0.04	1.1	0.51

[a] λ_{ex} = 300 nm, pH 6, μ = 0.2 M.

Table III: Global Analysis of [W126] Fluorescence Decay Data

λ_{em}	α_1[a]	α_2[a]	α_3[a]	$\langle\tau\rangle$	χ^2
320	0.257 ± 0.003	0.738 ± 0.003	0.006 ± 0.000	1.96	1.3
340	0.208 ± 0.003	0.784 ± 0.003	0.008 ± 0.001	2.03	1.1
360	0.192 ± 0.003	0.798 ± 0.003	0.010 ± 0.001	2.07	1.2
380	0.174 ± 0.003	0.809 ± 0.003	0.017 ± 0.001	2.12	1.1
400	0.165 ± 0.003	0.798 ± 0.003	0.037 ± 0.001	2.20	1.2
420	0.222 ± 0.004	0.697 ± 0.004	0.080 ± 0.002	2.25	1.2

[a] τ_1 = 0.80 ± 0.01 ns; τ_2 = 2.33 ± 0.005 ns; τ_3 = 5.64 ± 0.07 ns; global χ^2 = 1.2.

single-tryptophan proteins, collected as a function of emission wavelength, were analyzed in multiexponential and continuous distribution formats. Tables I and II summarize the results of the discrete exponential analysis. In general, it was found that the sum of three or four exponential terms was adequate to fit the data. Note that the χ^2 values are, in most cases, near unity, indicating a reasonable fit. An exception is the case of [W158][2] at 320- and 340-nm emission. Note that the average lifetime increases consistently with emission wavelength for all three proteins.

While the multiexponential fits in Tables I and II are acceptable, it is not clear that the decay components correspond in any sense to specific "species". To examine the possibility that there is such an association of lifetimes with physical species having different emission spectra, we performed global analyses on data collected as a function of emission wavelength with the lifetimes constrained to be the same for all emission wavelengths. The contribution of each species to the total fluorescence at the specified wavelength is determined by the preexponential factors (α_i's). Table III presents the results of a global analysis of the emission-dependent data for [W126]. The global χ^2 for this analysis is comparable to the unlinked analyses given in Tables I and II, and the standard deviations in the parameters are significantly smaller, both indicating that the lifetime linkage scheme is not unreasonable. The global analysis of data for the other two single-tryptophan variants, [W138] and [W158], with the same linkage scheme gave poor results with global χ^2 values of 1.7 and 2.4, respectively. The emission of [W126] appears to be adequately described by a model of several species present with different emission spectra and different lifetimes. In this case, the variation in the decay behavior with emission wavelength is very minor. The major effect is an increase in the amplitude of the long-lifetime component at longer wavelengths. This sense of the emission wavelength/lifetime component amplitude variation is also consistent with a relaxation model in which the long time

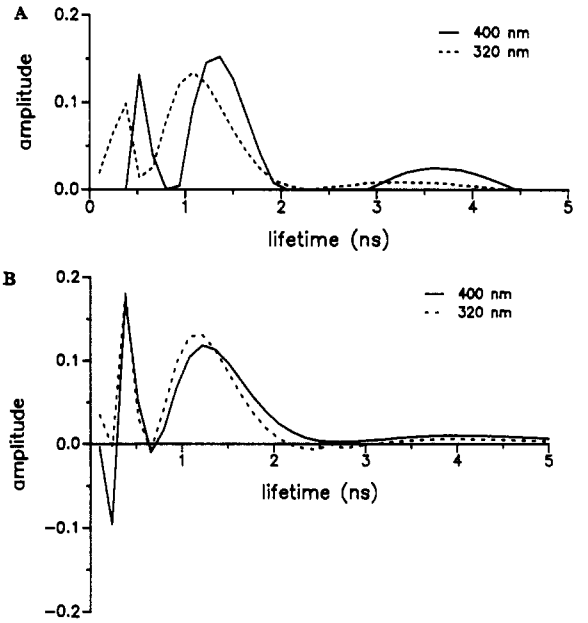

FIGURE 2: (A) James and Ware distribution analysis of [W138] at emission wavelengths of 320 (---) and 400 nm (—). The amplitudes have been constrained to be positive. (B) James and Ware distribution analysis of [W138] at emission wavelengths of 320 (---) and 400 nm (—). The amplitudes are not constrained.

[2] Notation: The modified forms of T4 phage lysozyme used in this study have one or two of the three tryptophan residues of the wild type replaced by tyrosine. We will refer to lysozymes containing one tryptophan as *single-tryptophan variants* and those containing two tryptophans as *double-tryptophan variants*. The notation used refers to the remaining tryptophan residues, e.g., [W126] = W138Y/W158Y where W138Y means that the tryptophan residue at position 138 has been replaced by tyrosine. [W126,W138] refers to a lysozyme with tryptophans W126 and W138 present. The notation without brackets, e.g., W138, refers to the residue at this position. The abbreviation T4L will commonly be used to denote T4 phage lysozyme. PLA_2 refers to (porcine) phospholipase A_2, and RNase T1 to (*Aspergillus oryzae*) ribonuclease T1.

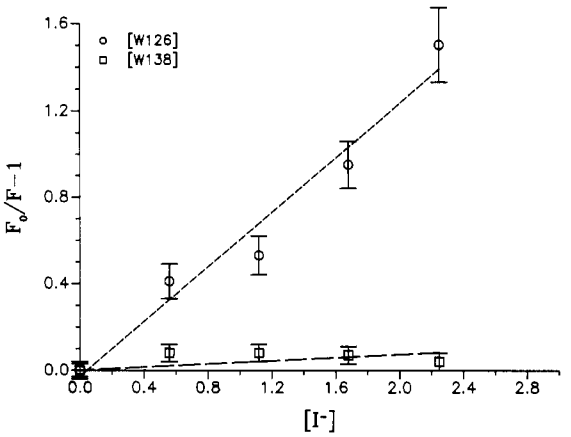

FIGURE 3: Stern–Volmer quenching plots. (○) [W126]; (□) [W138].

emission will necessarily be red shifted. In contrast, the nature of the underlying species description is more complex in the cases of [W138] and [W158]. It will be shown below that this has a rather simple interpretation in terms of the environments determining the photophysics of these tryptophans.

To determine whether the fluorescence data for these lysozymes containing single tryptophans could be better represented by a continuous distribution, we analyzed data sets using the James and Ware procedure described above. Figure 2A presents the results of a distribution analyses for the variant [W138] with amplitudes constrained to be positive (A) and unconstrained (B), respectively. We find in general that such analyses give as good χ^2 values as the sum of a few exponentials. The average lifetime values for the two methods of analysis are also comparable. This figure illustrates that the distribution analysis of wavelength-dependent emission data shows less dramatic changes than the specific α and τ parameters as a function of λ_{em} in a multiexponential analysis of three or four terms. There is a slight shift of parts of the overall distribution to longer lifetimes with increasing emission wavelength, and thus the average lifetimes from this analysis method show the same trend with emission wavelength as the multiexponential analyses. Figure 2B shows that if this analysis is performed with no constraints on the signs of the amplitudes, then on the red edge of the emission one finds a negative contribution at short lifetimes. The latter is indicative of a set of species generated as a result of excited-state reaction. Similar results are obtained for the other single-tryptophan variants. This behavior will be discussed in a subsequent publication.

Quenching Experiments at Constant Ionic Strength. Figure 3 shows Stern–Volmer plots for iodide quenching of the [W138] and [W126] lysozymes at a constant ionic strength of 2.3 M. The respective Stern–Volmer quenching constants are 0.012 M^{-1} for [W138] and 0.63 M^{-1} for [W126]. Using the average lifetimes of 1.4 and 2.0 ns, respectively, we deduce effective collisional quenching rate constants of 8.6×10^6 M^{-1} s^{-1} for [W138] and 3.2×10^8 M^{-1} s^{-1} for [W126]. The surface tryptophan in [W126] is quenched with a rate roughly an order of magnitude below the diffusion limit. In contrast, the buried tryptophan in [W138] is not significantly quenched by iodide. The [W158] lysozyme has a low quantum yield (see Table IV); it was not included in our KI quenching experiments. The bimolecular quenching constant of [W138] for acrylamide was determined to be 8.0×10^8 M^{-1} s^{-1}. This enhanced quenching efficiency for acrylamide versus iodide for buried residues has been previously noted (Somogyi et al., 1985; James et al., 1985). The reduction of the fluorescence intensity and the deduced bimolecular quenching constants were consistent with

Table IV: Quantum Yield and Average Lifetime Summary

variant/protein	$\langle\tau\rangle$	Q^a	k_r^b	k_{nr}^c
[W126]	2.0	0.060	0.030	0.47
[W138]	1.4	0.044	0.031	0.69
[W158]	0.40	0.013	0.033	2.47
[W126,W138]	1.30	0.039	0.030	0.74
[W126,W158]	1.10	0.030	0.027	0.88
[W138,W158]	0.80	0.030	0.038	1.22
WT	0.95	0.026	0.027	1.02

[a] Absolute quantum yields are relative to the value of 0.12 for tryptophan in aqueous solution at pH 6 from Chen (1972). [b] Radiative decay rate as calculated as $Q/\langle\tau\rangle$. Units are ns^{-1}. [c] Nonradiative decay calculated as $(1 - Q)/\langle\tau\rangle$. Units are ns^{-1}.

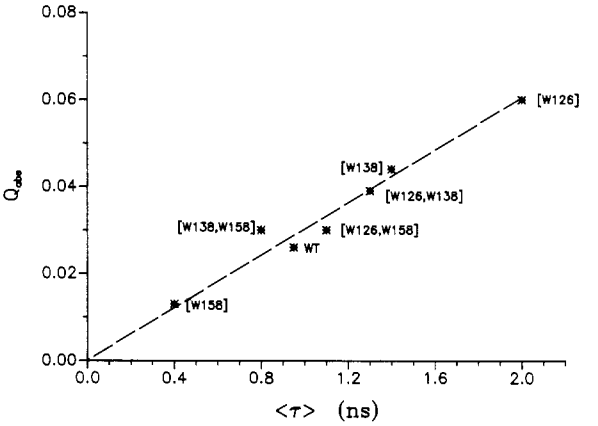

FIGURE 4: Plot of the quantum yield vs average lifetime for T4 phage lysozyme variants.

the effects of the added quenchers on the observed lifetimes of the single-tryptophan variants.

Relative Quantum Yields and Average Lifetimes. Table IV gives a summary of the average lifetimes and quantum yields for the single-tryptophan and several multi-tryptophan T4L variants. The values of the absolute quantum yields have been calculated relative to the quantum yield of tryptophan in aqueous solution at pH 6. For the single-tryptophan cases, the average lifetimes and quantum yields both increase in the order [W158] < [W138] < [W126]. A plot of quantum yield versus average lifetime is linear over a 3-fold change (Figure 4). This observed linearity implies that all three single-tryptophan variants have the same radiative rate constant and that this rate constant is the same for the proteins with two and three tryptophan residues. From the lifetime values for the variants involving substitutions of tyrosine for tryptophans, we have extracted radiative and nonradiative rate constants (Table IV). The radiative rate constant is found to be substantially the same for all proteins studied. The nonradiative rate constant shows considerable variation.

Multiexponential Analyses of T4L Variants Containing More than a Single Tryptophan. To determine what useful information can be gleaned from more complex cases, we have analyzed data which have emission components from more than one tryptophan. Table V summarizes these results. Our purpose in presenting these results is to show that one may obtain deceptively simple analyses for complex cases. While the lifetime and amplitude values extracted are not interpretable, the changes in average lifetimes deduced from such analyses may often be correlated with the effects of mutations on specific tryptophans. Dramatic examples of this are provided by variants Q105X where X = A or G. These variants have average lifetimes of ca. 3 ns compared to WT T4L which has an average lifetime of 0.95 ns (Table V). Such a large effect on the average value must be associated with an effect

Table V: Summary of Multiexponential Analyses of the Fluorescence Decays of T4L Variants Containing More than One Tryptophan and Wild Type[a]

variant/protein	α_1	τ_1	α_2	τ_2	α_3	τ_3	α_4	τ_4	$\langle\tau\rangle$	χ^2
[W126,W138]	0.214	0.127	0.445	1.12	0.233	1.86	0.108	3.3	1.3	1.1
	0.218	0.143	0.606	1.27	0.176	2.96			1.3	1.2
[W138,W158]	0.432	0.130	0.442	0.93	0.096	2.18	0.03	4.27	0.80	1.1
	0.444	0.146	0.482	1.03	0.074	3.42			0.82	1.3
[W126,W158]	0.410	0.232	0.232	0.797	0.329	2.08	0.028	4.06	1.04	1.2
	0.445	0.178	0.356	1.26	0.199	2.76			1.08	1.5
WT T4L	0.370	0.135	0.432	1.00	0.162	2.03	0.035	3.76	0.95	1.2
	0.380	0.150	0.514	1.14	0.106	2.99			0.96	1.2
Q105A	0.232	0.384	0.208	1.64	0.56	5.10			3.3	1.0
Q105G	0.241	0.345	0.258	1.70	0.50	4.56			2.8	1.0

[a] λ_{ex} = 300 nm; λ_{em} = 360 nm; T = 20 °C.

on individual residues that is at least as large.

Discussion

Correlation of Tryptophan Environment with "Simple" Spectral Parameters. The exposed areas of indole rings of tryptophan residues 126, 138, and 158 as calculated by the Richards and Lee procedure (Richards, 1977) using the WT structure (Weaver & Matthews, 1987) are 49, 7.5, and 33 Å^2, respectively. For reference, the total accessible surface area of a tryptophan side chain is 266 Å^2 using the same algorithm (probe radius of 1.6 Å; CHARMM van der Waals's radii). Note that W138 is a "buried" tryptophan while W126 and W158 are surface tryptophans with a large degree of exposure in aqueous solution. Consistent with this, the hydrogen exchange rate of the indole N–H of W138 is a factor of 20 slower than that of W126 and a factor of 40 slower than W158 at 10 °C (L. McIntosh, private communication; Phillips et al., 1988).

The quenching constant for I^- quenching of W126 and W138 is 3.2 × 10^8 and 8.6 × 10^6 M^{-1} s^{-1}. The relative magnitudes of the bimolecular quenching constants for iodide are consistent with the relative exposures deduced on the basis of the hydrogen exchange measurements, differing by a factor of 40 compared to 20 for the exchange rates. For comparison, the value for iodide quenching of indole in solution is 7 × 10^9 M^{-1} s^{-1} (Eftink & Ghiron, 1981) while that for the buried tryptophan of RNase T1 is 7.6 × 10^6 M^{-1} s^{-1} (James et al., 1985). Thus, the iodide quenching behavior demonstrates that W126 is largely exposed while W138 is almost as buried as the tryptophan of RNase T1. The same conclusion results from a comparison of the acrylamide quenching constants: 8 × 10^8 M^{-1} s^{-1} for [W138], 3.0 × 10^8 M^{-1} s^{-1} for RNase T1 (Eftink & Ghiron, 1975), and 7 × 10^9 M^{-1} s^{-1} for indole in solution (Eftink & Ghiron, 1981). Again, W138 is slightly more exposed than the buried tryptophan of RNase T1.

The photophysical behavior of a tryptophan residue should be determined by its environment, particularly the polarity and collisional quenching efficiency of the surrounding residues or solvent molecules. Figure 5 qualitatively compares the intrinsic polarity and quenching efficiency of the amino acid environments of the three tryptophan residues. The figure summarizes the distance of closest approach of polar functional groups to each of the tryptophans (nonpolar contacts, while numerous, are not indicated). Amino acids are labeled explicitly. The quenching efficiencies of the amino acids as determined from solution studies are also indicated symbolically. Crystallographically determined water molecules are not included. The contribution of water to the polarity of the tryptophan environment is best assessed from the Richards and Lee surface areas and quenching data discussed above.

W138 is hydrogen bonded to Q105 and a water molecule through the indole N–H. It is proximate to S136 and T142, and an arginine residue is within a 5-Å radius. W138 is in

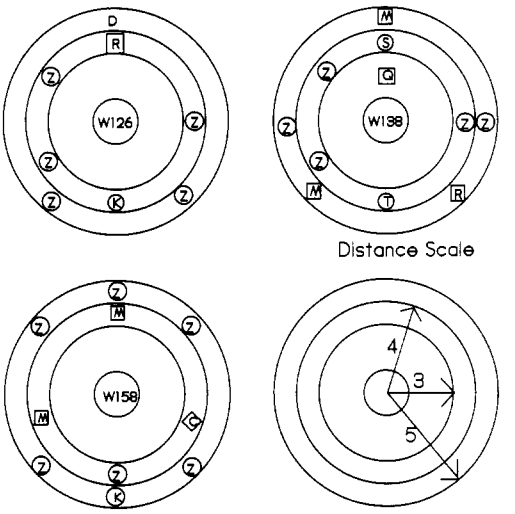

FIGURE 5: Amino acid environment of tryptophans in lysozymes. Quenching efficiencies are designated by (◇) strong, (□) moderate, (○) weak; Z = peptide functional groups. The circles are drawn at radii of 3, 4, and 5 Å from the center of the tryptophan residue.

a fairly polar amino acid environment for a buried hydrophobic residue. W126 is proximate to R95 and K124. W158 has M1, M6, and C97 as polar contacts. The surface tryptophans, W126 and W158, are exposed to solvent along the edges of their indole rings including the indole N–H. The contacts above and below the indole rings of the latter two tryptophans, however, are with amino acids. Note that all three tryptophans have numerous peptide contacts in the distance range from 3 to 5 Å.

The emission spectrum of tryptophan in proteins is generally a good indicator of the polarity of its environment. The Stokes shift of the ^1L_a state of tryptophan is quite sensitive to solvent polarity inasmuch as the excited-state dipole moment is much larger than the ground-state dipole moment. The λ_{max} values of the emission spectra of buried tryptophans in apoazurin (*Pseudomonas fluorescens*), parvalbumin, and RNase T1 are 308 nm (Szabo et al., 1983), 315 nm (Eftink & Hagaman, 1985), and 327 nm (James et al., 1985), respectively. Szabo and co-workers (Szabo et al., 1983) showed that the emission spectrum of apoazurin is identical with 3-methylindole in methylcyclohexane. The surface tryptophan in PLA_2 has a λ_{max} of 340 nm which blue shifts to 333 nm when the tryptophan inserts into a hydrophobic micellar environment (Ludescher et al., 1988). Similarly, the tryptophan of M13 coat protein in a micelle environment has a λ_{max} of 330 nm (Johnson & Hudson, 1989). Elwell and Schellman (1975) showed that the emission spectra of unfolded WT T4L enzyme and tryptophan in water are very similar ($\lambda_{max} \approx 350$ nm). Buried tryptophans rarely exist in an amino acid environment as apolar as apoazurin. Due to the polarity of the amino acid

environment or minute exposure to water, even buried residues usually have emission maxima as red as 333 nm.

The three tryptophans of T4L all have emission maxima of 330 nm. This has been determined by measuring the emission spectra of the three single-tryptophan variants (see Figure 1) using $\lambda_{ex} > 290$ nm to avoid tyrosine excitation. The identical nature of the spectra in the wild type has been confirmed by noting that iodide quenching of the WT surface tryptophan fluorescence results in no spectral shifts. When the criteria mentioned above are used, W138 of T4L is a buried tryptophan in a polar amino acid environment. The surface tryptophans, W126 and W158, have spectral shifts consistent with partial exposure of their indole rings to bulk solvent. These conclusions based on λ_{max}'s are consistent with the WT crystal structure (Weaver & Matthews, 1987). Mutations that alter the nonbonded contacts of W138 result in red-shifted emission spectra (Harris and Hudson, unpublished results). Thus, where present, differences in polarity are detectable.

For the purpose of discussion of photophysics, a "species" will be designated by a pair of rate constants (k_i^r, k_i^{nr}). If all of the processes that deactivate the excited state of indole derivatives are first order, then the observed quantum yield of each species is defined as

$$Q_i = \frac{k_i^r}{k_i^r + k_i^{nr}} = k_i^r \tau_i \quad (4)$$

where k_i^r and k_i^{nr} are the radiative and nonradiative rate constants of the ith species. The lifetime of each species is the inverse of the sum of these two rate constants. If the radiative rate constants associated with each species are the same, then the total intensity is

$$I(t) = P_0 k_r \sum_{i=1}^{n} \alpha_i \exp(-t/\tau_i) \quad (5)$$

where the α_i's sum to unity and P_0 represents the initial excited-state population. Under these circumstances, the quantum yield is

$$Q = k_r \sum_{i=1}^{n} \alpha_i \tau_i = k_r \langle \tau \rangle \quad (6)$$

In such a case, there is a linear relationship between quantum yield and average lifetime, and the radiative constant for all species is given by the ratio $Q/\langle \tau \rangle$.

The data in Table IV make possible a calculation of the radiative rate constant for each of the three tryptophans of T4L. Figure 4 shows that the three variants containing a single tryptophan have the same ratio of quantum yield to average lifetime since they fall on the same correlation line of Q vs $\langle \tau \rangle$. The most plausible explanation for this observation, given the significant difference in quantum yields and average lifetimes between the three single-tryptophan proteins, is that the radiative rate constants are the same for all three tryptophans. This is consistent with the observation of essentially identical emission spectra since variation in the radiative rate constant due to changes in the excited electronic state ordering or state admixture would be expected to lead to changes in the emission spectra. It is not surprising, given these results, that the proteins having two or three tryptophans also fall on the line in Figure 4. Because the T4 lysozymes containing single tryptophans have the same radiative rate constants, the factor responsible for the differences in the lifetime descriptions of the tryptophans in each of the three environments is variation of the nonradiative rates. The major nonradiative channel, we hypothesize, is collisonal quenching due to neighboring residues.

The radiative rate constant determined from the slope of the least-squares fit to the data in Figure 4 is $(2.9 \pm 0.3) \times 10^7$ s^{-1}. This corresponds to a radiative lifetime of 34 ± 4 ns. When the surface tryptophan of PLA_2, which has a radiative lifetime of ca. 58 ns in aqueous solution, is immersed in a hydrophobic micellar environment, its radiative lifetime is 34 ns (Ludescher, 1985). The radiative lifetimes of the buried tryptophans in RNase T1 (James et al., 1985) and apoazurin (Szabo et al., 1983) are 13 and 16 ns, respectively. This suggests, as do the emission spectra in Figure 1, that the tryptophans in T4L are in environments not quite as apolar as found for tryptophans in RNase T1 and apoazurin. This is consistent with the Richards and Lee surface exposures and the known amino acid polar contacts deduced from the crystal structure (see Figure 5). W138, for example, though it is buried, has several waters associated with it in the WT crystal structure, has numerous contacts with polar amino acids, and is somewhat quenched by acrylamide.

The collisional interactions of excited-state T4L tryptophan residues with neighboring amino acids may result in fluorescence quenching. To see if the trends in the nonradiative rate constants for the three tryptophan environments can be explained by the quenching efficiencies of neighboring amino acids, we have examined the bimolecular quenching constants for amino acids determined in solution. Such a correlation of solution and protein data is, in principle, limited by the fact that there is surely an orientational dependence to the efficiency of quenching. We confine our consideration of quenching efficiency to those amino acids that are moderate or strong quenchers, since it is likely that the quenching of those amino acids classified as weak quenchers probably is due to their α-COOH in solution studies. An attempt at such an environmental correlation is only possible where, as in this case, one has knowledge of the radiative rate constants for each tryptophan site.

Steiner and Kirby studied the intermolecular quenching of indole derivatives by a variety of substances, including several amino acids (Steiner & Kirby, 1969). We have determined the bimolecular quenching constants of *N*-acetyltryptophan by cysteine, glutamine, methionine, and asparagine.[3] Froehlich and Nelson (1978) found that amides, such as *N*-methyl- and *N*,*N*-dimethylacetamide, are very poor quenchers of substituted indoles ($k_q \sim 10^5$ M^{-1} s^{-1}). *N*-Alkyl-substituted formamides have bimolecular quenching constants of only $\sim 5 \times 10^7$ M^{-1} s^{-1}. Peptide linkages, as modeled by these compounds, are expected to be poor quenchers but certainly contribute to the polarity of the tryptophan environment.

We conclude, for the purpose of environmental correlations with photophysics, that cysteine and histidine are strong quenchers ($k_q > 10^9$ M^{-1} s^{-1}) and that glutamine, asparagine, methionine, and arginine (3×10^8 M^{-1} s^{-1} $\leq k_q < 5 \times 10^8$ M^{-1} s^{-1}) are moderate quenchers. This classification also agrees with Braams' (1966, 1967) characterizations of these amino acids in terms of electron scavenging abilities. The side chains of polar amino acids such as threonine and serine contribute to the polarity of the tryptophan environment in a protein but do not significantly quench tryptophan fluorescence. Studies of variants of T4L that interchange threonine for alanine as amino acid contacts of tryptophan-138 confirm that threonine

[3] The values of cysteine, glutamine, methionine, and asparagine were determined to be 1.8×10^9, 0.46×10^9, 0.48×10^9, and 0.41×10^9 ($\pm 0.5 \times 10^9$) M^{-1} s^{-1}.

has no significant quenching efficiency (Harris & Hudson, unpublished results). Peptides are at best weak quenchers of tryptophan fluorescence.

Figure 5 shows the distance distribution of polar amino acid contacts about the three tryptophans in T4L and indicates their relative quenching efficiencies. While the figure only includes residues up to 5 Å from each of the tryptophans, there are no quenchers significantly stronger than those indicated within 15 Å. Cysteine, glutamine, and arginine are the groups with greatest quenching efficiencies within short distances of tryptophan residues 158, 138, and 126, respectively. The presence of these groups within a few angstroms of the tryptophans makes them probable candidates for quenching interactions. On the basis of the bimolecular quenching constants and the distance correlations in Figure 5, one would expect the ordering of the quantum yields and average lifetimes of the single-tryptophan variants to be just as found in Table V, i.e., W126 > W138 > W158. Direct evidence for the conclusion that Q105 efficiently quenches W138 emission stems from the observation that the average lifetime of WT T4L is 0.95 ns while mutations that substitute inefficient quenchers for Q105 increase the average lifetime of such a multi-tryptophan variant by as much as a factor of 3 (Table V; Harris and Hudson, unpublished results).

Determination of the radiative rate for the single- and double-tryptophan variants as well as WT T4L in conjunction with the average lifetimes enables us to determine average nonradiative rate constants for this series. These are reported in Table IV. Note that the values are consistent with the major differences in quenching efficiency in the environments of the three tryptophans, i.e., $k_{nr}(W158) \gg k_{nr}(W138) > k_{nr}(W126)$. The ratios of the values of k_{nr} for the single-tryptophan variants in Table IV are approximately equal to the ratios of the bimolecular quenching constants of the amino acids that are closest to the respective tryptophans and have the highest quenching efficiency. In fact, the nonradiative rate constants for the groups 126/138/158 of 0.47/0.69/2.47 ns^{-1} are linearly related with a small positive intercept to the bimolecular quenching constants of the nearest effective quenching group Arg/Gln/Cys of 0.36/0.46/1.8 M^{-1} ns^{-1}. This, correlation strongly suggests that quenching makes a large contribution to the observed values of the nonradiative rate constants. Because of the preponderance of residues that are moderate to strong quenchers within short distances of the indole ring, the tryptophans of T4L have quantum yields that are less than half that of tryptophan in aqueous solution at the same pH (Chen, 1972). The correlation with the best quencher within a short distance works well for the weaker quenching environments of W126 and W138 because of the lack of strong quenchers at distances between 5 and 10 Å; the presence of strong quenchers such as cysteine or histidine within this distance range would probably complicate the analysis.

Examination of the temperature dependence of the nonradiative rate constants for the three single-tryptophan variants indicates Arrhenius-type behavior. The resulting activation energies were determined to be 8.5, 10.7, and 17.6 kJ mol^{-1} for [W158], [W138], and [W126], respectively. Given the magnitudes of these activation energies, it is likely that the quenching process involves the formation of a complex whose structure requires the alteration of amino acid side-chain orientations before the quenching can take place. The frequency factors associated with the activated processes are ca. 5×10^{10} to 5×10^{11} s^{-1}. These frequency factors are consistent with the encounter of the excited-state indole–quencher complex as a result of minor rearrangements of the protein prior to the charge transfer event. Such frequency factors are typical for condensed-phase reactive encounters within a "cage" where repeated collisions occur between the same pair of reactant molecules.

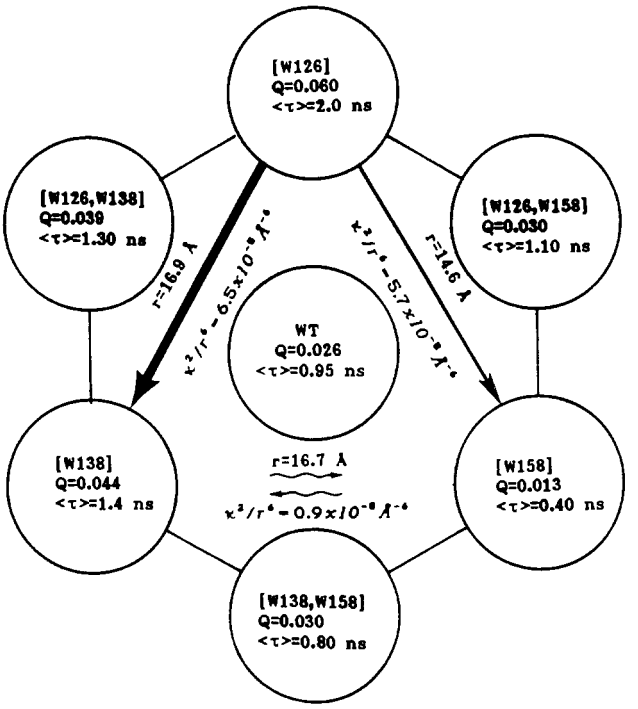

FIGURE 6: Summary diagram for lysozymes containing tryptophan to tyrosine substitutions and wild type. (Thickness of arrows between single-tryptophan variants indicates the relative magnitudes of Förster nonradiative energy transfer between pairs of tryptophans in double-tryptophan lysozyme variants.)

The relative quantum yields for lysozymes containing two tryptophans, given in Table IV, provide some information about energy transfer between residues in these proteins. The results are summarized in Figure 6. The quantum yield of the two-tryptophan proteins will be the average of the quantum yields of the variants containing single tryptophans if there is no energy transfer. If the energy transfer is unidirectional and from the high to low quantum yield residue, the observed quantum yield will be lower than the average of the quantum yields of the single-tryptophan lysozymes. The predicted efficiency of energy transfer is proportional to κ^2/r^6 where k is a function of the angle between vectors defining the donor and acceptor emission and absorption transition moment directions and the angles between these vectors and the vector between the two chromophores (Förster, 1948); r is the inter-tryptophan distance. The inter-tryptophan distances were determined between the centers of the indole rings. The 1.7-Å resolution crystal structure of Weaver and Matthews (1987) was used to determine the tryptophan separations and relative orientations. The values of r and κ^2/r^6 are reported in Figure 6 for the transition moment directions corresponding to the ^1L_a direction determined by Yamamoto and Tanaka (1972).

The major point of interest is that while for the [W138,W158] species the relative quantum yield is accurately the average of that for the individual single-tryptophan proteins, the other two-tryptophan proteins have quantum yields that are either slightly ([W126,W158]) or significantly ([W126,W138]) below the average values of the corresponding single-tryptophan proteins. This experimental result has been confirmed through multiple experiments and an independent investigation (L. McIntosh, private communication). Similarly, the relative quantum yield of the WT protein is 33% lower than expected on the basis of the average of the three

single-tryptophan proteins (i.e., 0.026 vs 0.039). These reduced quantum yields for the multi-tryptophan cases might be attributed either to perturbation of one site by Trp → Tyr substitution at the other or to energy transfer from the higher to the lower quantum yield residue. The possibility that the results for [W126,W158] and [W126,W138] are primarily due to the effect of substitution at one tryptophan site influencing another seems unlikely given that in the case of [W138,W158] the quantum yield is accurately the average of that for [W138] and [W158]. On the other hand, the magnitude for [W126,W138] is slightly lower than the quantum yield of W138, even with consideration of 10% quantum yield uncertainties indicating that there may be minor effects of site substitution perturbations.

We conclude on the basis of the quantum yield measurements that there is appreciable energy transfer from W126 to W138 and less efficient transfer from W126 to W158 but little if any net transfer from W138 to W158. The relative magnitudes of energy transfer between each of the pairs of tryptophans are in qualitative agreement with the magnitudes of κ^2/r^6 reported in Figure 6.[4] Ghosh et al. (1988) studied phosphorescence and optically detected magnetic resonance spectra of the same variants at 4.2 and 1.2 K. These authors invoke singlet–singlet energy transfer between tryptophans to explain their ODMR and phosphorescence intensity results. They conclude that there is significant energy transfer between W126 and W158 and minor energy transfer between W126 and W138. The spectra of [W138,W158] clearly indicated the lack of energy transfer between the tryptophans in this variant. These results and those derived from fluorescence data agree as to the pairs of tryptophans between which energy transfer occurs and as to the direction of transfer. The two methods differ in the relative magnitudes of energy transfer for the two "active" pairs.

Ghosh and co-workers (Ghosh et al., 1988) pointed out that their phosphorescence results can be explained by values of κ^2 consistent with donor and acceptor transition moment directions corresponding to that of the ^1L_b transition, which lies ca. 40° with respect to the long axis of the indole ring and nearly parallel to the C_β–C_γ bond. The results from their phosphorescence and our fluorescence studies are consistent with the known properties of the temperature dependence of the excited singlet states of indole derivatives in solution. As time increases after excitation, solvent relaxation about the initially prepared excited state results in a time-dependent shift of the ^1I_a state to lower energies. At sufficiently long times after excitation, the energy of the ^1L_a state is comparable or is lower than the ^1L_b state. In the absence of the contribution of reorientational components of the medium, as is the case at 4 K phosphorescence work, one expects the ^1L_b state to remain the low-lying excited singlet electronic state (Lami, 1981; Meech et al., 1982; Gudgin-Templeton & Ware, 1984). In contrast, at 293 K, as in our study, one expects the ^1L_a to be the emitting state. The apparent reversal of the relative energy-transfer efficiencies of [W126,W138] and [W126,W158] between the two studies is thus comprehensible, and the κ^2/r^6 values determined from the appropriate transition moment models for each case are consistent with the observed data.

Correlation of Fluorescence Decay Behavior with Tryptophan Environment. The results of analysis of T4L single-tryptophan lysozyme fluorescence decay data are complex as regards explicit parameterization in a multiexponential framework (see Tables I and II). Analyses based on sums of exponentials adequately fit the data with regard to the criteria of χ^2, Poisson weighted residuals, and runs tests. Yet, success in modeling the fluorescence decay behavior is not an indication that the parameters extracted in such analyses correspond to real species. A direct indication of this is that the more complex cases of multi-tryptophan variants can be adequately fit by an exponential fit involving three or four terms. Clearly in these cases, there is not a one-to-one correspondence between tryptophan states and lifetime parameters inasmuch as the single-tryptophan variants themselves require three or more terms. Furthermore, global analyses of data sets using a species–lifetime linkage model fail to give reasonable self-consistent fits for emission-dependent data in two of the single-tryptophan variant cases. A plausible explanation for the failure of such a simple species-linked analysis is that the underlying mixture of species are greater in number and complexity than is formulated in such a simple multiexponential species analysis. In general, a distribution analysis such as proposed by James and Ware fits the data as well as multiexponential analysis of T4L fluorescence data. The appearances of such analyses give some credence to the conception that there is a continuous distribution of lifetimes (see Figure 2A) associated even with tryptophans that are buried, and therefore immobilized, in a protein. The terms if a multiexponential analysis fit the major peaks in the distribution analysis and, as such, fit the overall distribution in an approximate manner. The addition of further exponential terms improves χ^2 only slightly and defines minor features in the overall underlying distribution.

If the constraint of having positive amplitudes in a James and Ware analysis is removed, then negative preexponentials, associated with the kinetics of formation of emitting species, are resolved for data obtained on the red edge of the emission (see Figure 2b). For these cases, the use of an unconstrained analysis results in a reduced χ^2. Unconstrained James and Ware analyses on blue edge emission data do not resolve significant negative amplitudes (Figure 2B) and result in the same or worse χ^2 values than when the amplitudes are constrained to be positive. Such analyses, while indicative of dipolar relaxation, are not as well determined as analyses methods using fewer parameters either which include aspects of dipolar relaxation in a model-linked manner (Harris and Hudson, unpublished results) or which use maximum entropy methods to eliminate spurious correlation between extracted parameters (Siemiarczuk & Ware, 1989; Livesey et al., 1986).

The decided advantage of the James and Ware distribution analysis is that it reveals that large changes in the parameters of a multiexponential analysis as a function of emission wavelength may be due to slight shifts of the distribution (see Figure 2). The parameters extracted from a multiexponential analysis of two to three terms merely fit different parts of the distribution at different wavelengths. The disadvantage of this analysis method is that it does not allow one to be any more specific about the interpretation of its parameterization in terms of the origins of the photophysical complexity than the simple multiexponential analyses. One cannot simply interpret the shape or position of the peaks in the recovered distribution plots.

The lifetime heterogeneity observed for each tryptophan in this protein is due to heterogeneity in the nonradiative channels. This may be seen by considering the magnitude of the second moments of the lifetime distributions which are on the

[4] The energy-transfer efficiency should also depend on the spectral overlap integral usually designated J. We have omitted this factor in our calculations. Within the limits of error, this factor appears to be the same for all six donor–acceptor combinations.

order of 0.5 ns^2 and noting that the nonradiative rate constants for each of the tryptophans are large compared to the radiative rate constant (see Table IV). Variations in nonradiative rate constants must comprise greater than 90% of the observed lifetime heterogeneity if the radiative lifetimes are in a range which is physically reasonable for tryptophan or indole derivatives in any environment (i.e., 10–70 ns). The complexity in the fluorescence decays is thus due to a large number of radiating species in microstates having a range of nonradiative rate constants. In the limit of a large number of such species, one obtains a continuous distribution.

CONCLUSIONS

The complexity of excited-state lifetime descriptions of tryptophans in T4 phage lysozyme arises from a heterogeneous set of nonradiative rate constants. The nonradiative rate constants extracted are large compared to the radiative rate constant. In this system, it has been possible to obtain a semiquantitative correlation of amino acid environment and quenching efficiencies with the magnitudes of the nonradiative rate constants observed. The values of the nonradiative constants and the magnitude of these quenching efficiencies are consistent with the notion that the contribution due to collisional quenching is larger than other nonradiative mechanisms. Energy-transfer rates in variants containing two tryptophans are found to be consistent with the known crystal structure and the premise that emission from the tryptophans in T4L is predominantly from the ^1L_a.

Because tryptophan is a large amino acid, when it is found buried in a tryptophan it is often fairly immobile. This is the case with at least one of the tryptophans in T4L. Because of the lack of internal motion of this buried tryptophan and its complex lifetime description, we have concluded that it is the detailed conformational state of the amino acids proximate to the tryptophan that is responsible for nonradiative rate constant heterogeneity. The states that give rise to this heterogeneity may differ in only minor ways as regards tryptophan side-chain torsional angles. Nonradiative processes such as dipolar relaxation and quenching do not require large-amplitude tryptophan motion. Many of these tryptophan states with different nonradiative rate constants do not interconvert rapidly on the time scale of the tryptophan excited-state lifetime because they require the rearrangement of several buried residues.

This depiction of tryptophan/protein states is merely a restatement of a concept of protein conformational substrates originally defined by Frauenfelder (Austin et al., 1974). As pointed out by Young (1988), there is a remarkable analogy between proteins and glasses from both the experimental and theoretical standpoints. Proteins have a quasi-degenerate ground state. This quasi-degeneracy arises in proteins because each amino acid has multiple interactions with adjoining residue atoms giving rise to two or more favored states resulting from these interactions. As such, the conformational energy surface for the system possesses many energy valleys that are separated by large barriers. The collection of nonradiative rate constants of tryptophan in such quasi-degenerate states gives rise to the observed excited-state lifetime complexity.

ACKNOWLEDGMENTS

We thank Lawrence McIntosh and Cynthia Phillips for the generous gifts of variants of T4L in which there have been substitutions of tyrosine for tryptophans and Joan Wozniak and Phillip Pjura for the gifts of Q105G and Q105A lysozymes. We especially thank Brian Matthews and Larry Weaver for providing coordinates of WT T4L, John Schellman, Walt Baase, and Wayne Becktel for helpful discussions regarding lysozyme stabilities, and Lawrence McIntosh for providing results of hydrogen exchange measurements and fluorescence spectra of T4L proteins.

Registry No. Tryptophan, 73-22-3; lysozyme, 9001-63-2.

REFERENCES

Alber, T., Grutter, M. G., Gray, T. M., Wozniak, J. A., Weaver, L. H., Chen, B. L., Baker, E. N., & Matthews, B. W. (1986) *UCLA Symp. Mol. Cell. Biol., New Ser. 39*, 307.

Alcala, J. R., Gratton, E., & Prendergast, F. G. (1987) *Biophys. J. 51*, 925.

Austin, R. H., Beeson, K., Eisenstein, L., Frauenfelder, H., Gunsalus, I. C., & Marshall, V. P. (1974) *Phys. Rev. Lett. 32*, 403.

Beechem, J., & Brand, L. (1985) *Annu. Rev. Biochem. 54*, 43.

Beechem, J. M., Amelroot, M., & Brand, L. (1985) *Anal. Instrum. 14*, 379.

Braams, B. (1966) *Radiat. Res. 27*, 319.

Braams, B. (1967) *Radiat. Res. 31*, 8.

Chen, R. F. (1972) *Res. Natl. Bur. Stand. 76a*, 593.

Chen, L. X.-Q., Longworth, J. W., & Fleming, G. R. (1987) *Biophys. J. 51*, 865.

Creed, D. (1984) *Photochem. Photobiol. 39*, 537.

Eftink, M. R., & Ghiron, C. A. (1975) *Proc. Natl. Acad. Sci. U.S.A. 72*, 3290.

Eftink, M. R., & Ghiron, C. A. (1981) *Anal. Biochem. 114*, 199.

Eftink, M. R., & Hagaman, K. A. (1985) *Biophys. Chem. 22*, 173.

Eftink, M. R., & Ghiron, C. A. (1987) *Biophys. J. 52*, 467.

Elwell, M., & Schellman, J. (1975) *Biochim. Biophys. Acta 386*, 309.

Förster, T. (1948) *Ann. Phys. (Leipzig) 2*, 55.

Froelich, P. M., & Nelson, K. (1978) *J. Phys. Chem. 82*, 2401.

Ghosh, S., Zang, L.-H., & Maki, A. G. (1988) *J. Chem. Phys. 88*, 2769.

Gonzalo, I., & Montoro, T. (1985) *J. Chem. Phys. 89*, 1608.

Grinvald, A., & Steinberg, I. Z. (1974a) *Biochemistry 13*, 5170.

Grinvald, A., & Steinberg, I. Z. (1974b) *Anal. Biochem. 59*, 583.

Grütter, M. G., Weaver, L. H., Gray, T. M., & Matthews, B. W. (1983) in *Bacteriophage T4* (Matthews, C. K., Kutter, E., Mosig, G., & Berget, P., Eds.) p 356, American Society of Microbiology, Washington, D.C.

Gryczynski, I., Eftink, M. R., & Lakowicz, J. R. (1988) *Biochim. Biophys. Acta 954*, 244.

Gudgin-Templeton, E. F., & Ware, W. R. (1984) *J. Phys. Chem. 88*, 4626.

Hershberger, M. V., Lumry, R., & Verrall, R. (1981) *Photochem. Photobiol. 33*, 609.

Hudson, B., Harris, D., Gray, T., & McIntosh, L. (1987a) *Biophys. J. 51*, 419a.

Hudson, B., Ludescher, R. D., Ruggiero, A., Harris, D. L., & Johnson, I. (1987b) *Comments Mol. Cell. Biophys. 4*, 171.

James, D. R., & Ware, W. R. (1985a) *Chem. Phys. Lett. 120*, 450.

James, D. R., & Ware, W. R. (1985b) *Chem. Phys. Lett. 120*, 455.

James, D. R., & Ware, W. R. (1986) *Chem. Phys. Lett. 126*, 7.

James, D. R., Demmer, D. R., Steer, R., & Verral, R. E. (1985) *Biochemistry 24*, 5517.

Johnson, I. D., & Hudson, B. S. (1989) *Biochemistry 28*, 6392.
Lakowicz, J. R., Szmacinski, H., & Gryczynski, G. (1988) *Photochem. Photobiol. 47*, 31.
Lami, H., & Glasser, N. (1986) *J. Chem. Phys. 84*, 597.
Livesey, A. K., Licinio, P., & Delaye, M. (1986) *J. Chem. Phys. 84*, 5102.
Ludescher, R. D., Volwerk, J. J., de Haas, G. H., & Hudson, B. (1985) *Biochemistry 24*, 7240.
Ludescher, R. D., Peting, L., Hudson, S., & Hudson, B. (1987) *Biophys. Chem. 28*, 59.
Ludescher, R. D., Johnson, I. D., Volwerk, J. J., de Haas, G. H., Jost, P. C., & Hudson, B. (1988) *Biochemistry 27*, 6618.
MacKerell, A. D., Jr., Rigler, R., Nilsson, L., Hahn, U., & Saenger, W. (1987) *Biophys. Chem. 26*, 247.
Mattes, S. L., & Farid, S. L. (1984) *Science 226*, 917.
Meech, S. R., & Phillips, D. (1983) *Chem. Phys. 80*, 317.
Meech, S. R., Phillips, D., & Lee, A. G. (1982) *Chem. Phys. Lett. 92*, 523.
O'Connor, D. V., & Phillips, D. (1984) *Time Correlated Single Photon Counting*, Academic Press, London.
Petrich, J. W., Chang, M. C., McDonald, D. B., & Fleming, G. R. (1983) *J. Am. Chem. Soc. 105*, 3824.
Petrich, J. W., Longworth,J. W., & Fleming, G. R. (1987) *Biochemistry 26*, 2711.
Phillips, C. L., McIntosh, L. P., & Dahlquist, F. W. (1988) *Biophys. J. 53*, 73a.
Richards, F. M. (1977) *Annu. Rev. Biophys. Bioeng. 6*, 151.
Ruggiero, A. J., & Hudson, B. S. (1989) *Biophys. J. 55*, 1111.
Siemiarczuk, A., & Ware, R. (1989) *J. Phys. Chem. 93*, 7609.
Somogyi, B., Papp, S., Rosenberg, A., Seres, I., Matko, J., Welch, R., & Nagy, P. (1985) *Biochemistry 24*, 6674.
Steiner, R. F., & Kirby, E. P. (1969) *J. Phys. Chem. 73*, 4130.
Szabo, A. G., & Rayner, D. M. (1980) *J. Am. Chem. Soc. 102*, 554.
Szabo, A. G., Stepanik, T. M., Wayner, D. M., & Young, N. M. (1983) *Biophys. J. 41*, 233.
Tanaka, F., & Mataga, N. (1987) *Biophys. J. 51*, 487.
Weaver, L. H., & Matthews, B. W. (1987) *J. Mol. Biol. 193*, 189.
Yamamoto, Y., & Tanaka, J. (1972) *Bull. Chem. Soc. Jpn. 45*, 1362.
Young, R. D. (1988) in *The Time Domain in Surface and Structural Dynamics* (Long, G. J., & Frandgean, F., Eds.) p 107, Kluwer Academic Publishers, New York.

Characterization of Particulate Cyclic Nucleotide Phosphodiesterases from Bovine Brain: Purification of a Distinct cGMP-Stimulated Isoenzyme

Seiko Murashima, Takayuki Tanaka, Steven Hockman, and Vincent Manganiello*
Laboratory of Cellular Metabolism, National Heart, Lung, and Blood Institute, National Institutes of Health, Bethesda, Maryland 20892

Received June 28, 1989; Revised Manuscript Received January 9, 1990

ABSTRACT: In the absence of detergent, ≈80–85% of the total cGMP-stimulated phosphodiesterase (PDE) activity in bovine brain was associated with washed particulate fractions; ≈85–90% of the calmodulin-sensitive PDE was soluble. Particulate cGMP-stimulated PDE was higher in cerebral cortical gray matter than in other regions. Homogenization of the brain particulate fraction in 1% Lubrol increased cGMP-stimulated activity ≈100% and calmodulin-stimulated ≈400–500%. Although 1% Lubrol readily solubilized these PDE activities, ≈75% of the cAMP PDE activity (0.5 μM [^{3}H]cAMP) that was not affected by cGMP was not solubilized. This cAMP PDE activity was very sensitive to inhibition by Rolipram but not cilostamide. Thus, three different PDE types, i.e., cGMP stimulated, calmodulin sensitive, and Rolipram inhibited, are associated in different ways with crude bovine brain particulate fractions. After solubilization and purification by chromtography on cGMP–agarose, heparin–agarose, and Superose 6, the brain particulate cGMP-stimulated PDE cross-reacted with antibody raised against a cGMP-stimulated PDE purified from calf liver supernatant. The brain enzyme exhibited a slightly greater subunit M_r than did soluble forms from calf liver or bovine brain, as evidenced by protein staining or immunoblotting after polyacrylamide gel electrophoresis under denaturing conditions. Incubation of brain particulate and liver soluble cGMP-stimulated PDEs with V_8 protease produced several peptides of similar size, as well as at least two distinct fragments of ≈27 kDa from the brain and ≈23 kDa from the liver enzyme. After photolabeling in the presence of [^{32}P]cGMP and digestion with V_8 protease, [^{32}P]cGMP in each PDE was predominantly recovered with a peptide of ≈14 kDa. All of these observations are consistent with the existence of at least two discrete forms (isoenzymes) of cGMP-stimulated PDE.

Cyclic nucleotide phosphodiesterases (PDEs) constitute a complex group of enzymes, which are found in varying amounts and proportions in different mammalian cells and tissues (Beavo et al., 1982). At least six or seven distinct types or classes of PDEs can be distinguished on the basis of their subcellular localization, biochemical, pharmacological, immunological, and physical properties, and regulatory mechanisms. Representatives of several types (Beavo, 1988), i.e., Ca^{2+}- and calmodulin-sensitive PDE (Kincaid et al., 1984), cGMP-stimulated PDE (Martins et al., 1982; Yamamoto et al., 1983a; Miot et al., 1985; Pyne et al., 1986; Whalin et al., 1988), cGMP-inhibited PDE (Grant & Coleman, 1984; Harrison et al., 1986; Degerman et al., 1987), and rod outer segment PDE (Baehr et al., 1979), have been extensively

* To whom correspondence and reprints requests should be addressed at the National Institutes of Health, Building 10, Room 5N-307, 9000 Rockville Pike, Bethesda, MD 20892.